Simulation of the Performance of Various PFPE lubricants under Heat Assisted Magnetic Recording conditions

Mohammad Soroush Ghahri Sarabi
David B. Bogy
Department of Mechanical Engineering
University of California, Berkeley

May 30, 2014

Abstract

In this study, we perform simulations for the Z-tetraol family of lubricants with 4 hydroxyl end-groups, including Z-tetraol 1200 as a low molecular weight member of the family and Z-tetraol 2200 as a high molecular weight of the family, and also for ZTMD with 8 hydroxyl group as a multidentate lubricant, which is manufactured based on the Z-tetraol family. All studies are performed for 4 cases of lubricant thicknesses including 5, 7, 12, and 14A. These numbers are chosen in order to have a fair comparison with a previous study for Z-dol. We also investigate the relative effects of evaporation with respect to the thermocapilary shear stress. It is found that after a 2ns illumination of the laser, a trough and two side ridges across the down-track direction can be seen in the lubricant. The performances of the lubricants can be ranked mainly based on the trough depth and also evaporation such that better lubricants show less deformation and trough depth under equal conditions of thermal spot size and peak temperature.

1 Introduction

In the proposed future hard disk drive (HDD) magnetic recording technology known as Heat Assisted Magnetic Recording (HAMR), there are several difficult head-disk interface issues to be addressed and solved. A key issue among those corresponds to the behavior of the polymer lubricant that coats the HAMR recording media. The lubricants, which are mostly from the perfluoropolyether (PFPE) family of lubricants, are ideally supposed to cover the HAMR media uniformly. However, several events can occur in which the lubricant layer deforms, or depletes, and subsequently, it loses the ideal shape and this can decrease the stability of the slider's flying attitude over the disk, which may

cause a decrease in the performance and reliability of the Head Disk Interface (HDI). Therefore, several efforts have been reported in the litrature to improve the performance of the lubricants via optimization of the molecular structure of the basic lube designs such as Fomblin Z. Such efforts introduced new molecular structures such as the Z-dol and Z-tetraol families which include hydroxyl polar end-groups as well as multi-dentate lubricants such as ZDMD and ZTMD which also include hydroxyl groups in the middle of the molecule chains (Figure 1) [11]. This specific design of the lubricants gives them the special ability to bond to the Diamond Like Carbon (DLC) substrate. This also changes the behavior of their disjoining pressure, viscosity, and vapor pressure.

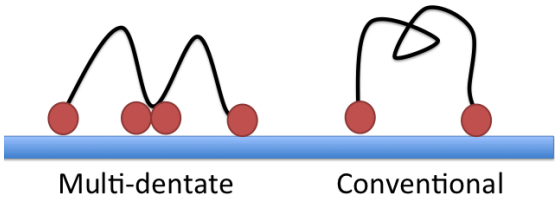

Figure 1: Molecular structure of a typical multi-dentate lubricant like ZTMD versus the molecular structure of a conventional End-Group Functional lubricant like Z-dol and Z-tetraol. The red beads represent the active hydroxyl (-OH) group that has a polar interaction with DLC layer [11]

Among simulation analyses performed on lubricant behavior under HDI situation, two groups of studies stand out. First it must be noted that the typical value for lubricant film thickness is of the order of 1nm which is almost equal to the characteristic size of the lube molecules; therefore, one can argue that the use of Molecular Dynamics models seems to be more legitimate than continuum models since the lubricant is almost in a monolayer regime. On the other hand, the other length scales of the problem such as the HAMR laser spot size, around 20nm, and slider's characteristic size around 800um, give more credence to the idea of modeling the lubricant as a continuum to have a more cost effective analysis. Specially, the separation of length scales in this problem implies the use of lubrication theory for a Newtonian fluid as a first order approximation, even though the PFPE lubricants' behaviors are viscoelastic and nonlinear. Many researchers found that the mentioned method can describe the behavior of the PFPEs very well; specifically, Scarpulla et al. [6], and Marchon and Saito [8] report that the continuum model can agree well with experiments and the much more expensive Molecular Dynamics simulations. Also, one can follow the trail of the continuum model in former research studies such as Wu [9], and Dahl and Bogy [12]. This study is mostly based on the assumptions made by Dahl and Bogy in which the lubricant is assumed to have an unknown thickness h(x,y;t), pressure p(x,y;t) and shear stress $\tau(x, y; t)$ which are functions of thickness h as well as x, y, and t. In the following sections, the functionality of pressure on h will be discussed. Also for this thin film case, an effective viscosity is assumed

that takes into account the effects of temperature and lubricant thickness. The viscoelasticity effects of the lubricant will be the subject for future studies.

2 Problem Definition

The evolution equation of the lubricant according to the lubrication theory can be written as (see figure 2):

$$\frac{\partial h}{\partial t} + u_D \frac{\partial h}{\partial x} + \frac{\partial}{\partial x}\left[-\frac{h^3}{3\eta}\frac{\partial p}{\partial x} + \frac{h^2}{2\eta}\tau_x\right] + \frac{\partial}{\partial y}\left[-\frac{h^3}{3\eta}\frac{\partial p}{\partial y} + \frac{h^2}{2\eta}\tau_y\right] + \frac{\dot{m}}{\rho} = 0 \quad (1)$$

where h is the unknown lubricant thickness, u_D is the disk velocity in the down-track x-direction, which is assumed in this study to be a constant of 5m/s, η is the lube effective viscosity, p is the pressure, τ_x and τ_y are the shear stresses in x and y directions, ρ is the density assumed to be a constant, $\dot{m}$ is the mass flux corresponding to the evaporation. In this study, the lubricant thicknesses of 5, 7, 12, and 14A are considered for the Z-tetraol family of lubricants as well as for ZTMD as a representative for multi-dentate lubes. This choice of lubricant thicknesses is made in order to have a fair comparison with previous work on the lubricant Z-dol 2000 by Dahl and Bogy [12]. Also, with the same reasoning and in order to simulate the situation close to the actual HAMR operation, the laser spot is assumed to be a Gaussian temperature distribution with maximum temperature of 350^oC and a Full Width Half Maximum of 20 (nm).

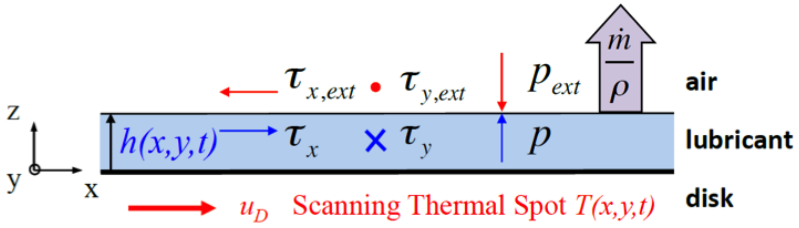

Figure 2: HAMR lubricant write process schematic: The thin lubricant film of unknown thickness h(x,y;t) is subject to a scanning laser spot of speed u_D, which is represented by a prescribed Gaussian temperature distribution T(x,y;t). Lubricant flow is driven by the resulting external shear stresses $\tau_{x,ext}$ and $\tau_{y,ext}$ and pressure gradient$(\nabla p)_{ext}$. Some lubricant is also removed from the film via mass evaporation $\dot{m}$.

The Fomblin Catalog [15] suggests that the density of all PFPEs including Z-dol and the Z-tetraol family are almost the same, therefore in this study, we assume the same density value for all lubricants in order to simplify the comparison. However, each lubricant has a different behavior of viscosity, disjoining pressure, and evaporation. These parameters can typically be functions of molecular weight, lubricant thickness, temperature, and number of hydroxyl groups in the molecular structure. The following sections outline the estimations

used here on effective thin-film viscosity of each lubricant as functions of lube thickness, disjoining pressure as a function of lubricant thickness, and evaporation as a function of molecular weight, lube thickness, and temperature. It's also worthwhile to introduce the surface tension and discuss how it is connected to the problem in terms of Maragoni and thermocapillary shear stress.

2.1 Surface Tension Effects

Surface tension has two important effects on the physics of this problem. The first effect is a force normal to the interfacial element of the liquid which is caused by the curvature of the surface element. This normal force is often called Laplace pressure and can be described as

$$p_{Laplace}\boldsymbol{n} = -\gamma(\nabla.\boldsymbol{n})\boldsymbol{n} = \gamma(\nabla^2 h) \tag{2}$$

The second effect of surface tesion becomes visible when a non-uniform distribution of surface tension is present on the liquid-gas interface. In this study, this phenomenon happens because of the Gaussian temperature distribution, and the surface tension highly depends on the temperature. Therefore, there is a tangential shear force exerted on the interfacial element, which is called Maragoni or thermocapillary shear stress, and it is of the form

$$\boldsymbol{\tau} = \boldsymbol{\nabla}\gamma - \boldsymbol{n}(\nabla\gamma.\boldsymbol{n}) \tag{3}$$

where $\boldsymbol{n}$ is the normal vector to the interface and $\boldsymbol{\nabla}$ is the two dimensional gradient operator $\boldsymbol{\nabla} = \frac{\partial}{\partial y}\boldsymbol{e_x} + \frac{\partial}{\partial y}\boldsymbol{e_y}$. In our configuration the normal unit vector $\boldsymbol{n}$ can be considered fully vertical and assumed to be $\boldsymbol{n} = \boldsymbol{e_z}$, therefore the second term in equation 3 is negligible. So, we can write the equations 2 and 3 as

$$p_{Laplace}\boldsymbol{n} = \gamma(\nabla^2 h)\boldsymbol{e_z} \tag{4}$$

$$\boldsymbol{\tau} = \boldsymbol{\nabla}\gamma = \frac{\partial\gamma}{\partial y}\boldsymbol{e_x} + \frac{\partial\gamma}{\partial y}\boldsymbol{e_y} \tag{5}$$

The surface tension of a non-polar PFPE lubricant was measured in the limited temperature range of $10 - 180^oC$ and found to be linear [10]. Dahl and Bogy [12] assume that functional PFPE lubricants such as Zdol have a similar slope, and in their model, they use the slope $\partial\gamma/\partial T = -0.06mN/(m^oC)$. The same assumption is made here for the Z-tetraol family of the lubricants. Under these assumptions, we can rewrite the equation 5 as

$$\boldsymbol{\tau} = \boldsymbol{\nabla}\gamma = \frac{d\gamma}{dT}\frac{\partial T}{\partial y}\boldsymbol{e_x} + \frac{d\gamma}{dT}\frac{\partial T}{\partial y}\boldsymbol{e_y} \tag{6}$$

where the spatial derivatives of temperature can be found from the prescribed temperature $T(x, y)$.

2.2 Surface Energy and Disjoining Pressure

For thin films, the liquid-air and liquid-solid interfaces come so close to each other that the interaction between them cannot be neglected. The interaction between these two interfaces happens via the disjoining pressure. For non-polar lubricants like Fomblin Z, disjoining pressure is limited only to a dispersive component which has van der Waals sources. While, for polar lubricants, a term of polar disjoining pressure should also be considered whose source is the polar interactions between the hydroxyl end-groups of the lube molecules and the DLC substrate. Disjoining pressure can generally be a function of molecular weight, lubricant thickness, and the production process of the lubricants, e.g. annealing. The disjoining pressure can be expressed in the form of a point-wise normal force that is exerted to a surface element of the liquid-air interface. Such a force causes a difference between the pressure of the liquid and pressure of the outer air as follows

$$\Pi(h) = p - p_\infty \tag{7}$$

where $\Pi(h)$ is the disjoining pressure as a function of h, p is the liquid pressure, p_∞ is the air pressure out side of the liquid. Many researchers tried to obtain an appropriate expression for the surface energy and disjoining pressure of PFPE lubricants. Waltman and Deng [14] give expressions for the surface energies of Z-tetraol 1200 and Z-tetraol 2200. Guo et al. [11] give an expression for the surface energy of the ZTMD for both components of dispersive and polar. Karis and Tyndall [5] give an accurate expression for the disjoining pressure of the Z-dol as well. One can use the surface energy of the lubricant to find the disjoining pressure as a function of lube thickness according to the equation:

$$\Pi(h) = -\frac{\partial \gamma}{\partial h} = -\frac{\partial \gamma^d}{\partial h} - \frac{\partial \gamma^p}{\partial h} = \Pi^d(h) + \Pi^p(h) \tag{8}$$

In order to fit a curve to the experimental data of surface energy, Karis uses a general form of

$$\gamma^d = \frac{A_{eff}}{12\pi} \frac{1}{(d_0 + h)^2} + \gamma_\infty \tag{9}$$

for the dispersive component of the surface energy of Z-dol 2000; where γ_∞ is the bulk surface energy and A_{eff} is the effective Hamacker constant. Some scholars define the Hamacker constant in the equation above using a $1/24\pi$ instead of $1/12\pi$. For convenience, we converted all Hamacker constants in the different references to the standard form of equation 9 and included these numbers in table 1 Also, for the polar component of surface energy of this lubricant, Karis uses a polynomial expansion of degree 7 as:

$$\gamma^p = \sum_{n=0}^{7} a_n \left(\frac{h}{d_1} \right)^n \tag{10}$$

with the curve fitting parameters a_n and d_1 stated in table 1. We made the same curve fitting assumptions for Z-tetraol 1200, Z-tetraol 2200, and ZTMD

and obtained the curve fitting parameters for these lubricants, which are also available in this table. The surface energy and disjoining pressure of the four different lubricants, Z-dol 2000, Z-tetraol 1200, Z-tetraol 2200, and ZTMD are plotted against the lube thickness in figures 3 and 4, respectively.

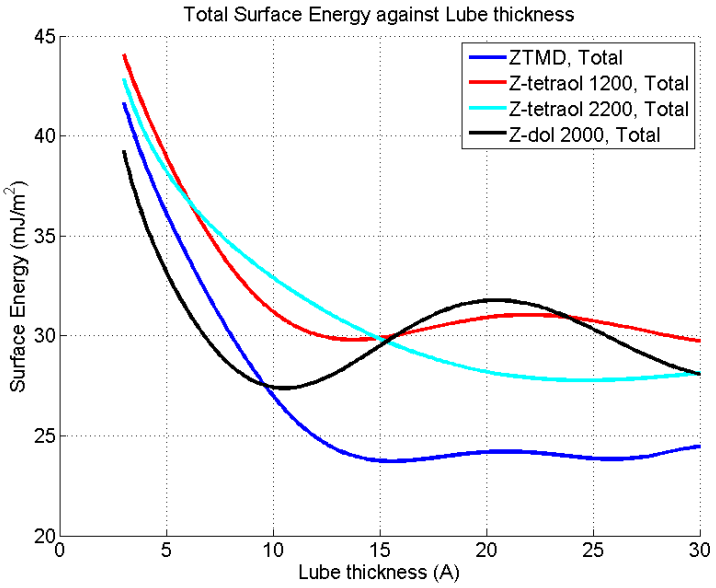

Figure 3: Total surface energy as a function of lubricant thickness for Z-dol 2000, Z-tetraol 1200, Z-tetraol 2200, and ZTMD. Surface Energy Parameters are calculated for both dispersive and polar components of the disjoining pressure for these lubricants according to Karis [5], Waltman and Deng [14], and Guo et al. [11]

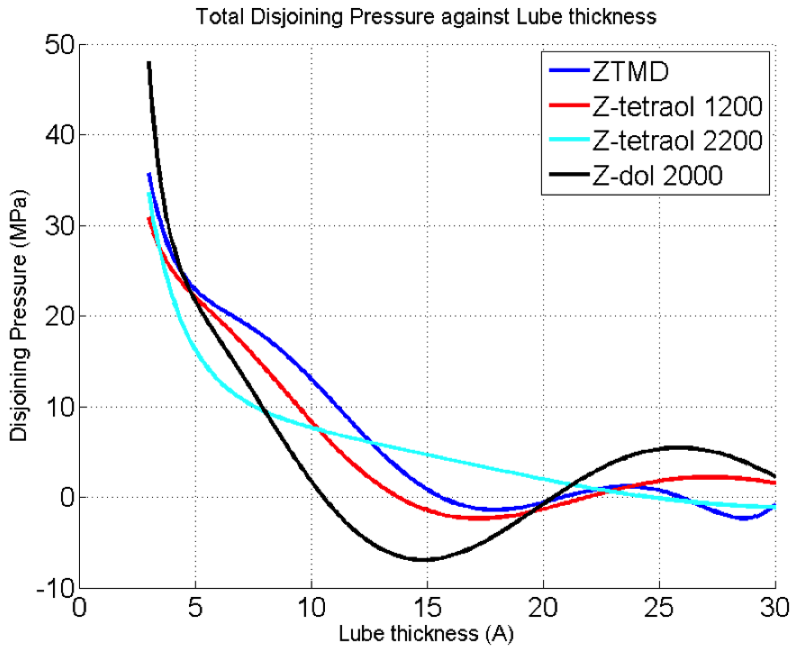

Figure 4: Total disjoining pressure as a function of lubricant thickness for Z-dol 2000, Z-tetraol 1200, Z-tetraol 2200, and ZTMD. It's noticable that ZTMD and Z-tetraol 1200 have a close disjoining pressure and critical lubricant thickness (where the disjoining pressure derivative is zero). This graphs are obtained accrding to the equation 8 differentiating the surface energy function with respect to the lubricant thickness.

One should also pay attention to the disjoining pressure derivative in figure 4. In this figure, the disjoining pressure for 4 cases of lubricants is obtained via differentiating the surface energy with respect to lubricant thickness according to equation 8. In the governing equation, the disjoining pressure gradient $\nabla\Pi$ plays the role of the restoring force. Using the chain rule, we can rewrite this gradient, $\nabla\Pi$, in terms of lubricant thickness gradient, ∇h

$$\nabla\Pi = \frac{\partial\Pi}{\partial h}\nabla h \tag{11}$$

Therefore, the disjoining pressure gradient works as a restoring force only if $\frac{\partial\Pi}{\partial h}$ is negative. This is true for all PFPE lubricants shown in figure 4 under a critical lubricant thickness. This critical thickness is about 15, 17, 30, and 18A for Z-dol 2000, Z-tetraol 1200, Z-tetraol 2200, ZTMD respectively.

Parameters	Z-dol 2000	Z-tetraol 1200	Z-tetraol 2200	ZTMD
A_{eff}	2.36e-20	1.05e-19	0.95e-19	1.6e-19
d_0	0	2.5e-10	2.5e-10	3.1e-10
d_1	4e-10	2.5e-10	2.5e-10	3.1e-10
γ_∞	26e-3	14e-3	14e-3	13e-3
a_0	0.35634428	0.9678459291	1.5128571428	1.1213629434
a_1	0.943984495	0.9879638948	-0.0152365170	0.3506537679
a_2	-1.09056649	-0.6222581529	-0.0222572384	-0.0706675084
a_3	0.493599274	0.1562738262	0.0020998962	-0.1177336448
a_4	-0.10894144	-0.0197097888	6.8099856129e-05	0.0530550632
a_5	0.0125571518	0.0013264714	-1.4464249241e-05	-0.0089188687
a_6	-7.28088361e-4	-4.5559179547e-05	5.5575615663e-07	6.7622826254e-04
a_7	1.68021545e-5	6.2845783870e-07	-6.5130218754e-09	-1.9387479410e-05

Table 1: Surface Energy Parameters for Z-dol 2000, Z-tetraol 1200, Z-tetraol 2200, and ZTMD according to Karis [5], Waltman and Deng [14], and Guo et al. [11]

2.3 Thin-film effective viscosity

In order to have a good estimation of the thin-film effective viscosity of each lubricant, we must first have a good estimation about the bulk behavior of the material. Then one can introduce assumptions on how and why the viscosity of lubricant in the thin-film model is different. Karis [7] gives estimates of the bulk viscosity behavior of the Z-dol and Z-tetraol families of lubricants. In order to describe the bulk viscosity of the thin-film as a function of temperature, he applies the Eyring's rate theory to the PFPE lubricants and provides the equation

$$\eta(T) = \frac{N_A h_P}{V_l} exp(\frac{\Delta E^*_{vis} - T\Delta S^*_{vis}}{RT}), \tag{12}$$

which describes the viscosity as a function of temperature in which N_A, h_P, and V_l are Avogadro's number, Planck's constant and the molar volume of the lubricant, which can be calculated based on its molecular weight and density as:

$$V_l = \frac{M_w}{\rho} \tag{13}$$

Also, in equation 12, the terms ΔE^*_{vis} and ΔS^*_{vis} are key parameters, the so called activation flow energy and entropy, respectively. Karis finds the ΔE^*_{vis} and ΔS^*_{vis} for Z-dol and Z-tetraol using a curve fitting method on the experimental data of bulk viscosity of these materials as functions of temperature. So, by using two constants of ΔE^*_{vis} and ΔS^*_{vis}, we are able to express the bulk viscosity as a function of temperature. Guo et al. report some experimental

data of bulk viscosity of ZTMD as a function of temperature, as shown in figure 5. So, we can fit a curve using the Eyring's theory on these experimental data and find the activation flow energy and entropy for ZTMD. Figure 5 shows the curve fitted on ZTMD experimental viscosities versus temperature. Also, the bulk viscosities of Z-dol and Z-tetraol lubricants are shown in this figure. Therefore, we can summarize the bulk activation flow energy and entropy for

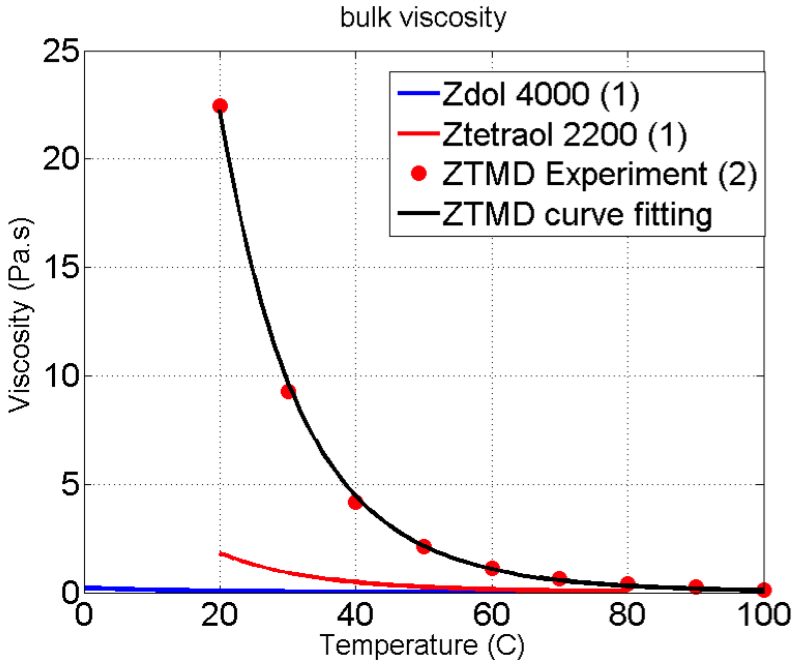

Figure 5: Bulk viscosity as a function of temperature for 3 different type of lubricants including Z-dol, Z-tetraol and ZTMD. It is clear that ZTMD has a greater visocsity compared to Z-tetraol and Z-tetraol compared to Z-dol.

Z-dol, Z-tetroal and ZTMD in table 2.

Lubricant	$\Delta E^*_{vis}[KJ/mol]$	$\Delta S^*_{vis}[J/molK]$
Z-dol	34.7	9.87
Z-tetraol	50.8	44
ZTMD	61.4	59.2

Table 2: Bulk activation flow energy and entropy for different materials

The next step in establishing an accurate model for the physics of this problem is to amend the bulk viscosity model to a viscosity that also takes into account the effect of the thin-film regime. Karis et al. state that the ΔE^*_{vis} and

ΔS^*_{vis} for bulk liquids can be amended to a new form of activation flow energy and entropy as a function of lubricant thickness as follows

$$\Delta E_{vis}(h) = \Delta E^*_{vis} - \frac{\mu(h)}{n} \tag{14}$$

where$\Delta E_{vis}(h)$ is the activation flow energy for the thin film as a function of lubricant thickness h. ΔE^*_{vis} is the activation flow energy of the bulk material mentioned above, μ is the chemical potential, which is a function of the dispersive component of the disjoining pressure and the molar volume as follows

$$\mu(h) = V_l \Pi^d(h) \tag{15}$$

Also, it is worth noting that n in equation 14 is the ratio of activation evaporation energy to activation flow energy as follows:

$$n = \frac{\Delta E^*_{Evap}}{\Delta E^*_{vis}} \tag{16}$$

Physically speaking, the activation evaporation energy is equivalent to the energy needed to remove a molecule from the system of molecules and fill the remaining hole with the remaining liquid molecules; while, the activation flow energy is equivalent to the energy needed to move a molecule among other molecules. Normally, the ratio n between these two activation energies is around 3 to 5 depending on the molecular weight of the liquid and other factors. The ΔS^*_{vis} corresponding to the bulk material can also be amended to a new form of $\Delta S_{vis}(h)$ which is a function of lubricant thickness h; however, it is observed [4] that under a specific lubricant thickness of 2nm, $\Delta S_{vis}(h)$ is constant for the Z-dol familiy. The term $\Delta S_{vis}(h)$ corresponds to the arrengement of the molecules and how this arrangement changes with the change in the state of the system. The arrangement of the molecules on a DLC substrate, and how they change during shearing, is almost the same for all types of PFPE lubricants that exhibit a spaghetti-like long carbon chain and polar end-groups that are attached to the disk. Therefore, we can assume that $\Delta S_{vis}(h)$ is constant for Z-tetraol and ZTMD lubricants as well. So according to Karis, we can write the new activation entropy as the sum of the bulk value and a correction term as:

$$\Delta S^{thin}_{vis}(h) = \Delta S^*_{vis} + \Delta \tilde{S}(h) \tag{17}$$

Where $\Delta \tilde{S}(h) = 0$ for bulk material where h is large and $\Delta \tilde{S}(h)$ is constant for $h < 2nm$. Using a number of try and errors, we found that we can assume the same amount of $\Delta \tilde{S}(h)$ for different PFPE lubricants. Such a choice, gives the most optimized amendment of thin to bulk viscosity ratio $\eta(h)/\eta_\infty$. Assuming all these thin-film modifications, we amend the Eyring's theory to a new form that accomodates the effect of lubricant thickness. Therefore, with a slight change, we can rewrite the equation 12 in the form of

$$\eta(T,h) = \frac{N_A h_P}{V_l} exp(\frac{\Delta E_{vis}(h) - T\Delta S^{thin}_{vis}}{RT}) \tag{18}$$

Then using this equation, we can find the viscosity model for 3 different types of lubricants, Z-dol, Z-tetraol, and ZTMD. Figure 6 shows the viscosity versus lubricant thickness for different temperatures for all 3 different types of lubricants. The viscosity shown in this figure for Z-dol has been used in former studies such as Karis [7] and Dahl and Bogy [12]; however, no published data is found for the viscosity of thin-film Z-tetraol and ZTMD. The viscosities found and shown in figure 6 for Z-tetraol and ZTMD are estimated based on above explanations. In order to have a comparison of the viscosity of Z-teraol and ZTMD with that for Z-dol, we plot in figure 7 the ratio of the viscosity between Z-tetraol and Z-dol as well as ZTMD and Z-dol. According to figure 7, the viscosity ratio of Z-tetraol to Z-dol changes between 1 and 80; also, the viscosity ratio of ZTMD to Z-dol is between 10 and 4000.

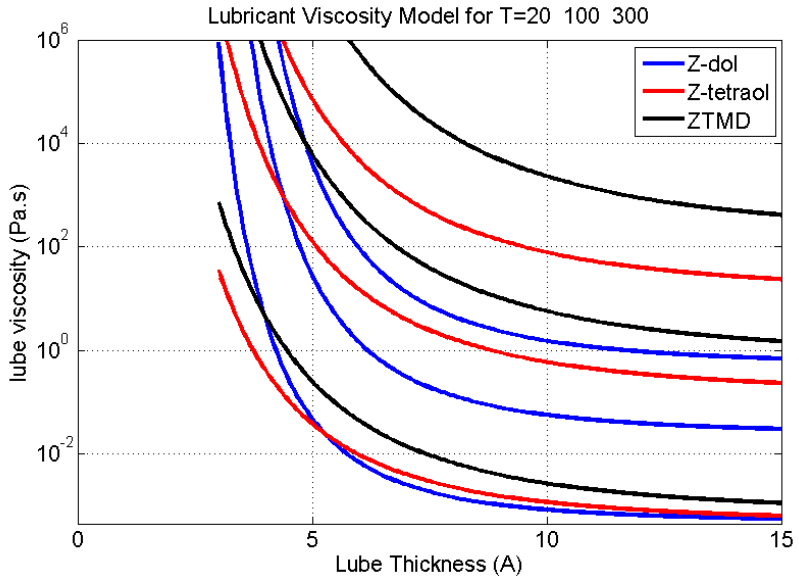

Figure 6: Thin-film effective viscosity as a function of lubricant thickness for different temeratures for different lubricants. For each lubricant, 8 graphs are plotted corresponding to viscosity as a function of temperatures: $T = \{20, 100, 300^oC\}$. Higher curves correspond to temperatures lower temperatures (closer to room temperature)

One may argue that such viscosity ratios are too high for lubricants that share the same structure. However, experiments on lubricant reflow show that this estimation is reasonable and the viscosity of Z-tetraol and ZTMD are far higher than Z-dol. Specifically, Mate [13] studied the spreading of droplets of PFPE lubricants on unlubricated, carbon-overcoated disk surfaces. He reports the time needed for a droplet to spread over the disk and reports that as the number of hydroxyl groups on a molecular structure increases from zero, for

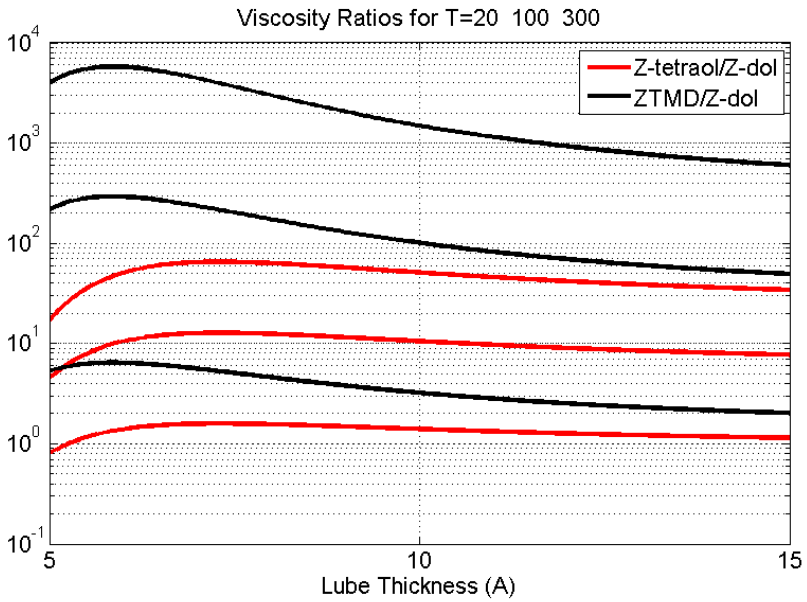

Figure 7: Thin-film effective viscosity ratio of Z-tetraol to Z-dol and ZTMD to Z-dol as a function of lubricant thickness for different temeratures for different lubricants. This is a comparison between these families of lubricants at temperatures $T = \{20, 100, 300^oC\}$. Higher curves correspond to lower temperatures (closer to room temperature)

Fomblin Z, to two for Z-dol, to four for Z-tetraol, to eight for ZTMD, the spreading time dramatically increases, which indicates the strong decrease in mobility of the lubricant and subsequently, a drastic increase in the effective viscosity. Therefore, such a high value of viscosity for Z-tetraol and ZTMD compared to Z-dol agrees with the experimental work by Mate.

2.4 Evaporation

The same approach that was used for viscosity of a thin-film is used for evaporation. First, we introduce bulk evaporation properties of the materials and explain how we estimate them. Second, we will use the disjoining pressure properties of the material to calculate the evaporation properties of the thin films. Finally, we can find the mass flux due to evaporation using the obtained data. The mentioned approach has been used in former studies by Dahl and Bogy [12] and Karis [7]; however, previous works only estimate the properties for the Z-dol family of lubricants but do not give any estimation about newer lubricants such as the Z-tetraol family and ZTMD. Generally speaking, the vapor pressure of PFPEs depends on many factors. Among those the temperaure, molecular weight, activation evaporation energy and entropy are the most im-

portant factors. Therefore, we can write the vapor pressure of the liquid in the form of $P^*_{vap} = p(M_w, T, \Delta E^*_{vap}, \Delta S^*_{vap})$. Karis applied the Clapyron equation to get an estimation for vapor pressure of the pure liquid lubricant, which can be represented as

$$P^*_{vap} = p_0 exp(\frac{-\Delta E^*_{vap} - T\Delta S^*_{vap} + RT}{RT}) \tag{19}$$

One should also note that for bulk liquids, the activation evaporation energy and entropy are functions of molecular weight and temperature. For the Z-dol family of lubricants, experimental measurements on vapor pressure exhibit a linear relation between the molecular weight and the activation evaporation energy. Karis mentioned that this relation for Z-dol has the form

$$\Delta E^*_{vap}[KJ/mol] = 50 + 29M_w[Kg/mol] \tag{20}$$

which comes from the comparison between the simulated data and the experimental data obtained from thermogravimetric analysis (TGA). However, there is no useful accurate experimental information about the Z-tetraol family of lubricants. So, we need to somehow get an estimation about this key parameter in order to have a good prediction about the bulk vapor pressure of the Z-tetraol as well as ZTMD. To find an expression for activation evaporation energy of the Z-tetraol family, we make the same assumption of a linear relation between ΔE^*_{vap} of Z-tetraol and its molecular weight M_w, with two unknown parameters of β_1 and β_2 to be determined, and we write

$$\Delta E^*_{vap} = \beta_1 + \beta_2 M_w \tag{21}$$

By comparing the equation above with equation 20, one can see that $\beta_1 = 50KJ/mol$ and $\beta_2 = 29J/gr$ for the Z-dol family of lubricants.

The physics of evaporation and viscosity are very close to each other. In evaporation, some energy is injected into the system to activate the molecules to escape from the liquid phase. In viscosity, the activation energy is needed for molecules to overcome the bonds and van der Waals forces between liquid and substrate molecules, and in the case of thin-film shear motion, move along the disk. So, there must be a quantitative relation between these two activation energies. Equation 16 illuminates this relation in terms of a parameter n. According to the litrature [7], the parameter n should be in the range of 3 to 5 depending on the lubricant's molecular weight for this class of lubricants (For Z-dol between 2.3 and 4.8). So we can formulate an inequality for Z-tetraol:

$$2.3 \leq n = \frac{\Delta E^*_{Evap}}{\Delta E^*_{vis}} \leq 4.8 \tag{22}$$

Our calculations show that we can extract two limits of low molecular weight $M_w = 1200Da$ and high molecular weight $M_w = 4000Da$ for this inequality and write

$$\Delta E^*_{vap} = \beta_1 + \beta_2 M_w = 2.3\Delta E^*_{vis} \qquad M_w = 1.2[Kg/mol] \tag{23}$$

$$\Delta E^*_{vap} = \beta_1 + \beta_2 M_w = 4.8\Delta E^*_{vis} \qquad M_w = 4[Kg/mol] \tag{24}$$

Solving this system of equations and knowing $\Delta E^*_{vis} = 50.8[KJ/mol]$ for Z-tetraol, we obtain the parameters $\beta_1 = 61KJ/mol$ and $\beta_2 = 45.7J/gr$.

Researchers and engineers have a tendency to use longer and heavier molecule chains in lubricant design to supress the effect of evaporation as much as possible; but, there is a trade-off between disjoining pressure properties and evaporation properties of the lubricants. According to Guo et al. [11], ZTMD as a multi-dentate lubricant, which is made of a couple of Z-tetraol short chain molecules (1000 Da), has the critical lube thickness and disjoining pressure properties close to Z-tetraol 1200; while, it should have the evaporation properties of Z-tetraol 2200. This claim apears to be legitimate because the disjoining pressure behavior of the ZTMD is close to that for Z-tetraol 1200 according to figure 4. And, the molecular weight and end-groups of ZTMD are close to those for Z-tetraol 2200. Therefore, it is reasonable to assume the same bulk evaporation properties for Z-tetraol 2200 and ZTMD in this study.

2.5 The Governing Equation and Boundary Conditions

Using the assumptions made so far, we can rewrite the lubrication equation (1) in the form

$$\frac{\partial h}{\partial t} + u_D \frac{\partial h}{\partial x} + \frac{\partial}{\partial x}\left[\frac{h^3}{3\eta}\frac{\partial}{\partial x}(\Pi(h) + \gamma\nabla^2 h) - \frac{h^2}{2\eta}c\frac{\partial T}{\partial x}\right] + \\ + \frac{\partial}{\partial y}\left[\frac{h^3}{3\eta}\frac{\partial}{\partial y}(\Pi(h) + \gamma\nabla^2 h) - \frac{h^2}{2\eta}c\frac{\partial T}{\partial y}\right] + \frac{\dot{m}}{\rho} = 0 \tag{25}$$

The spatial domain of the solution is a sufficiently large domain $[0 \leq x \leq X, 0 \leq y \leq Y]$ with the Dirichlet boundary conditions of $h = h0$ on the boundaries. It's also worthwhile to note that the terms of evaporation $\frac{\dot{m}}{\rho}$ and thermocapillary shear stress $\frac{h^2}{2\eta}c\frac{\partial T}{\partial x}$ play the role of the driving force in this governing equation while the terms of disjoining pressure and laplace pressure gradients $\frac{\partial}{\partial x}(\Pi(h) + \gamma\nabla^2 h)$ work as the restoring force of the system.

2.6 Numerical Scheme

The numerical scheme for solving this equation is a finite volume method that solves the nonlinear diffusion part of the system coupled with a Cubic Interpolation Propagation method (CIP) [2], [3] which solves the advection part of the problem. The numerical scheme is based on developments of H. Kubotera [1] and J. Dahl [12], former researchers of Computer Mechanics Laboratory.

3 Results

First we give a brief overview about the physics of the problem. The integrated HAMR system has a laser delivery system that conveys the energy to the magnetic layer and heats the target point above the Curie temperature in order to

perform a proper process of magnetic flux reversal and hence writing on the media. The lubricant coating on the disk will also be subjected to the high temperature and will start to deplete at the target point due to evaporation and thermocapilary shear stress. We investigate the problem of evoltion of lubricant thickness under laser illumination. The physics of heat transfer from the Near Field Transducer (NFT) to the magnetic media and the reverse heat transfer from media to NFT are still a matter of some controversy and are not well understood. In order to avoid such complication, we prescribe a Gaussian temperature distribution on the disk and therefore on the lubricant with a full width half maximum (FWHM) close to that of the so called laser spot. In this study FWHM is set to the goal of the hard disk industry which is 20nm. Also, the maximum temperature of the laser spot is set to 350^oC for all cases, and the ambient condition is $T_0 = 25^oC$ and $p_0 = 1atm$. In this study the effects of external shear stress and pressure from the air bearing are neglected since they change on a length scale of a few microns; while, in the laser spot the thermocapillary shear stress and disjoining and Laplace pressures change on a length scale of few nanometers (of the order of laser spot size). Therefore, the gradients of thermocapilary shear stress and disjoining and Laplace pressures at the laser spot are far higher compared to the mechanical shear stress and pressure from the air bearing, by a factor of a thousand.

3.1 Lubricant Depletion under HAMR conditions

In the previous study by Dahl and Bogy [12], they found the lubricant deformation for Z-dol 2000 with two hydroxyl end-groups for different maximum temperatures, different cases of disjoining pressure, and different possibilities for the evaporation model. In this study, we perform some simulations on the Z-tetraol family with 4 hydroxyl end-groups, including Z-tetraol 1200 as a low molecular weight member of the family and Z-tetraol 2200 as a high molecular weight of the family, and also, on ZTMD with 8 hydroxyl group as a multidentate lubricant which is manufactured based on Z-tetraol family. All studies are performed in 4 cases of lubricant thickness including 5, 7, 12, and 14A. These numbers are chosen in order to have a fair comparison with the previous study on Z-dol. We also investigated the relative effect of evaporation with respect to the thermocapilary shear stress. After a 2ns illumination of the laser, a trough and two side ridges along the down-track direction can be seen in the lubricant. Figure 8 gives a schematic depection of the trough and the side ridges. The performance of lubricants can be ranked mainly based on the trough depth and also evaporation such that better lubricants show less deformation and trough depth under equal conditions of thermal spot size and peak temperature. In order to obtain a better comprehension about the trough depth, this parameter is normalized by the initial lubricant thickness and is shown for different types of lubricant.

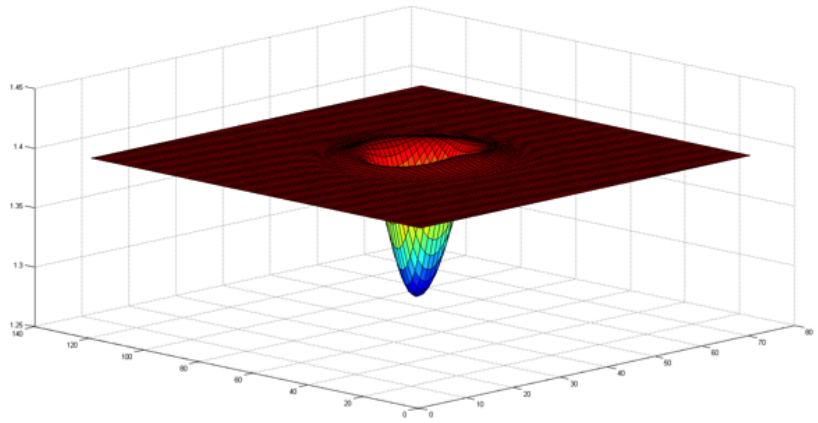

Figure 8: Schematic geometry of a lubricant depletion including trough and side ridges for a typical laser shine condition of 2ns illumination with 20nm laser spot and 350^oC peak temperature of the spot.

In figures 9, 10, 11, and 12, which we show the simulation results for 5, 7, 12, and 14A lubricant thicknesses respectively, the red part of each column represents the share of evaporation in lubricant depletion while the blue part shows the share of thermocapillary shear stress in lube depletion. Figure 9 shows a comparison bewteen the different lubricants with 5A initial lubricant thickness. For all 4 cases of lubricants at 5A, the deformation is less than 1% of the initial lubricant thickness, which is negligible.

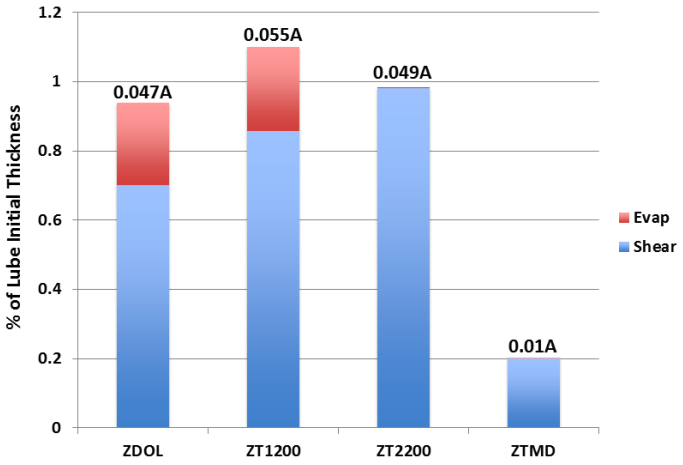

Figure 9: Trough Depth for different lubricants at 5A initial lubricant thickness, normalized and shown as the percent of initial lubricant thickness ($h_0 = 5A$). Also, the actual amount of depletion is mentioned above each column. In each column, the red part shows the share of the evaporation and blue part shows the share of thermocapillary shear stress.

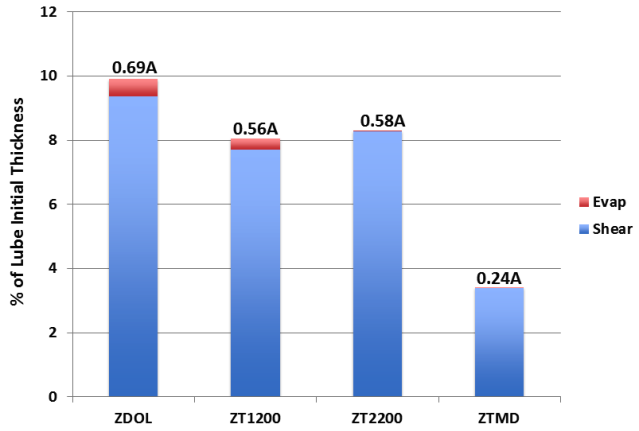

Figure 10: Trough Depth for different lubricants at 7A initial lubricant thickness, normalized and shown as the percent of initial lubricant thickness ($h_0 = 7A$). Also, the actual amount of depletion is mentioned above each column. In each column, the red part shows the share of the evaporation and blue part shows the share of thermocapillary shear stress.

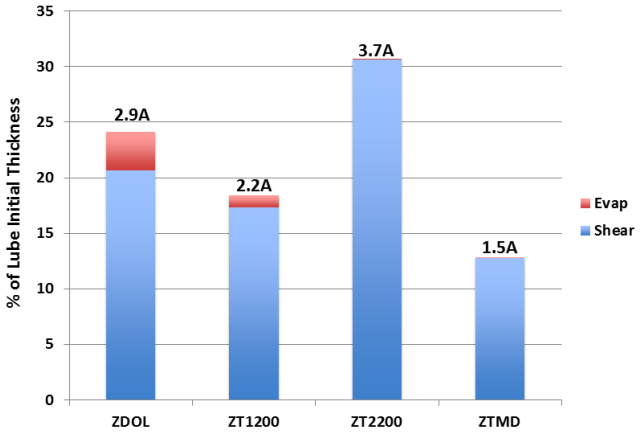

Figure 11: Trough Depth for different lubricants at 12A initial lubricant thickness, normalized and shown as the percent of initial lubricant thickness ($h_0 = 12A$). Also, the actual amount of depletion is mentioned above each column. In each column, the red part shows the share of the evaporation and the blue part shows the share of thermocapillary shear stress.

Figure 10 shows a comparison of the lubricant with 7A initial thickness. The deepest trough in this case belongs to Z-dol 2000 which has almost 10% of the intial thickness or 0.7A. Clearly, the deformation for the Z-tetraol family is around 8% of the initial thickness, which is less than the one for Z-dol. ZTMD exhibits 4% trough depth which is less than all other lubricants. This shows the superiority of the performance of ZTMD in sub-nanometer thin-film regimes. Figure 11 shows the analysis results for the 12A initial thickness case in which Z-dol shows a vulnerable behavior with a considerable trough depth of 2.9A, which is almost 25% of the initial thickness. Z-tetraol 1200 and ZTMD show less deformation in this case (2.2A and 1.5A respectively). However, Z-tetraol 2200 shows more deformation, 3.7A, which can be explained by its weaker disjoining derivative, according to figure 4. Again in this case, we can see that ZTMD shows a better performance. It has less evaporation, less lubricant mobility, and stronger disjoining pressure derivative compared to other lubricants which explain the performance of this lubricant.

For the 14A case of initial lubricant thickness, Figure 12 shows the same regime as seen in the 12A. In this case, Z-dol and Z-tetraol 2200 exhibit relatively large trough depths of 4.25A and 4.9A respectively, that are more than 30% of the initial thickness while the deformation for the Z-tetraol 1200 is less and it is still less than 2A for ZTMD. All four figures imply that ZTMD shows a better performance under HAMR conditions compared to the other types of lubricants. This behavior comes from its better bonding properties which leads to better viscosity, evaporation and disjoining pressure properties.

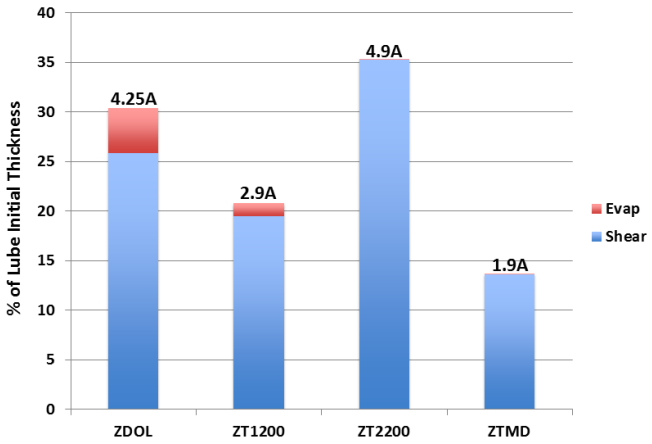

Figure 12: Trough Depth for different lubricants at 14A initial lubricant thickness, normalized and shown as the percent of initial lubricant thickness ($h_0 = 14A$). Also, the actual amount of depletion is mentioned above each column. In each column, the dark blue part shows the share of the evaporation and light blue part shows the share of thermocapillary shear stress.

In figures 9 through 12, each column has two portions. The light blue portion corresponds to the case when we suppress the effect of evaporation and study the effect of thermocapillary shear stress only. While, taking into account the effects of both thermocapillary shear stress and evaporation, we obtain the total trough depth (total amount of each column) for each case. Therefore, the difference between the total amount of each column and its blue portion gives the share of evaporation.

3.2 Evaporation under HAMR conditions

The share of evaporation for Z-dol 2000 and Z-tetraol 1200 is considerable in all cases of lubricant thickness. However, for the case of Z-tetraol 2200 and ZTMD the share of the evaporation is almost negligible in all cases. This behavior of lubricants can be described by the bulk vapor pressure of the materials. Z-dol 2000, according to equation 20, has an activation evaporation energy of $108 KJ/mol$. The value for Z-tetraol 1200 as a short chain molecule is $115.8 KJ/mol$ according to the equation 21. This value for Z-tetraol 2200 and ZTMD is $170.7 KJ/mol$ according to the same equation. Equation 18 shows the importance of the activation evaporation energy on the bulk pressure of the material; as ΔE^*_{vap} increases, the p_{vap} and, consequently, $\dot{m}$ decrease exponentially. Figure 13 also supports this argument since it shows a considerably low mass flux due to evaporation for cases of Z-tetraol 2200 and ZTMD.

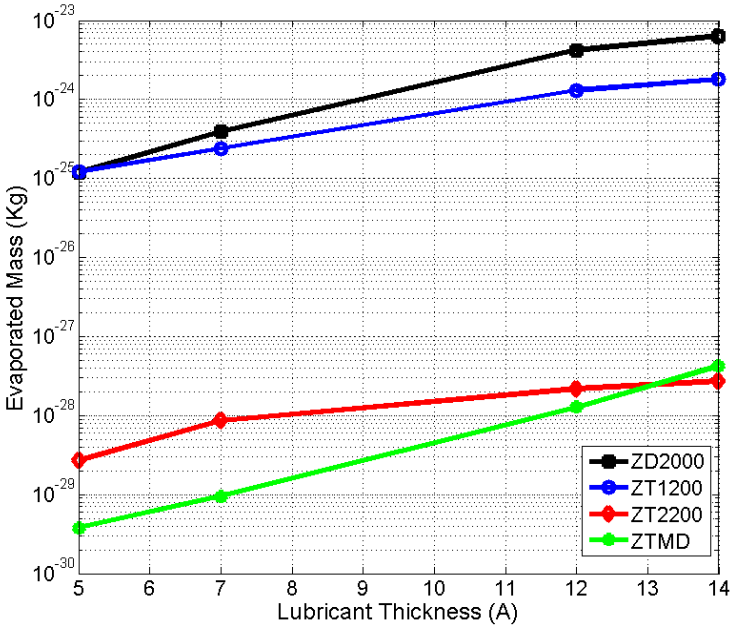

Figure 13: Evaporation as a function of lubricant thickness for different lubricants. As the lubricant thickness increases, the amount of evaporation also increases since lube molecules are less bonded to the disk and disjoining pressure decreases. ZTMD and Z-tetraol 2200 exhibit much less evaporation due to their smaller bulk evaporation pressure.

Hence, we can distinguish the thermocapillary shear stress as the main driving force for depletion in Z-tetraol 2200 and ZTMD; also, comparing the deformation of ZTMD with that for Z-dol and Z-tetraol illuminates the fact that this lubricant is more resistant against motion (due to its high viscosity and low mobility), and has stronger restoring force (due to disjoining pressure gradient).

The effect of molecular weight is also of interest here. Figure 13 implies that an increase in molecular weight from Z-tetraol 1200 to Z-tetraol 2200 decreases the evaporation by a factor of 10^{-4}; however, figure 4 shows that increasing the molecular weight not only increases the critical lubricant thickness from 17A for Z-tetraol 1200 to 30A for Z-tetraol 2200, but also it decreases the disjoining pressure derivative and therefore, weakens the restoring force of the lubricant, which is the disjoining pressure gradient in this case. That is the reason why Z-tetraol 2200 exhibits greater trough depths compared to Z-tetraol 1200. So, there is a trade-off in increasing the molecular weight of the Z-tetraol lubricant. As the molecular weight increases, the evaporation properties improve while disjoining pressure gradient becomes weaker making the lubricant more vulnerable against thermocapillary shear stress. These simulations also give insight into

the shape of the trough and side ridges. In cases where the evaporation is dominant, it is observed that the side ridges are smaller and in some cases no side ridges are found. This fact can be useful for future experiments on lubricant deformation under HAMR conditions.

4 Discussion

We found in this study that as the number of hydroxyl groups in a PFPE lubricant increases, some effects can be observed in the behavior of the lubricants, such as an increase in viscosity, a decrease in mobility, and a considerable decrease in evaporation; specifically, evaporation is almost turned off in case of Z-tetraol 2200 and ZTMD which agrees with experiments. As the molecular weight and the backbone chain length increase, a decrease in depletion due to evaporation can be observed as well as an increase in depletion due to disjoining pressure effects. Simulations predict relatively small depletion for ZTMD, which can be attributed to its evaporation and disjoining pressure properties and the mobility of this lubricant.

No experimental data could be found for 20 nm laser spots to be compared with the predictions of this study. Experimentalists prefer spot size ranges of the order of a few hundred nanometers due to the resolution of the Optical Spectrum Analyzers (OSA). However, this study reveals the effects of lubricant design parameters such as molecular weight and polar end-groups and their effect on disjoining pressure, viscosity, mobility, and evaporation properties of the lubricants, which alter the performance of the lubricant under HAMR conditions. It should also be observed that the Z-dol family of lubricants as well as Z-tetraol and ZTMD are conventional lubricants that don't accomodate the high temperature resistivity; therefore, thermal degradation might occur for these lubricants at larger temperatures. In order to avoid the controversies with regard to the thermal decomposition of the lubricants, we kept the peak temperature of the laser spot at a medium temperature of 350^oC. Another issue is the polydispersivity of the polymer molecules, which is not considered in this study since the experimental data about these lubricants are scarce, specifically for the Z-tetraol and ZTMD family.

5 Acknowledgement

This work was supported by the Computer Mechanics Laboratory at the University of California, Berkeley, Mechanical Engineering Department. The authors would also like to acknowledge the International Disk Drive Equipment and Materials Association (IDEMA) Advanced Storage Technology Consortium (ASTC) project for providing funding for this research.

References

[1] H. Kubotera and D. Bogy, "Numerical simulation of molecularly thin lubricant film flow due to the air bearing slider in hard disk drives," *Microsyst Technol, vol. 13, no. 8-10, pp. 859–865.* 2007.

[2] T. Yabe, T. Aoki, G. Sakaguchi, and P. Wang, "The compact CIP (Cubic-Interpolated Pseudo-particle) method as a general hyperbolic solver," *Computers & Fluids, vol. 19, no. 3-4, pp. 421-431.* 1991.

[3] T. Aoki, "Multi-dimensional advection of CIP (Cubic-Interpolated Propagation) scheme," *Computational Fluid Dynamics Journal, vol. 4, no. 3, pp. 279–291.* 1995.

[4] T.Karis, B.Marchon, V.Flores, and M.Scarpulla, "Lubricant spin-off from magnetic recording disks," *Tribology Letters, vol. 11, no. 3-4, pp. 151–159.* 2001.

[5] T. Karis and G. Tyndall, "Calculation of spreading profiles for molecularly-thin films from surface energy gradients," *Journal of Non-Newtonian Fluid Mechanics, vol. 82, pp. 287–302.* 1999.

[6] M. Scarpulla, C. Mate, and M. Carter, "Air shear driven flow of thin perfluoropolyether polymer films," *Journal of Chemical Physics, vol. 118, no. 7, pp. 3368–3375.* 2003.

[7] T. Karis, "Lubricants for the Disk Drive Industry," in Lubricant Additives: Chemistry and Applications, L. Rudnick, Ed. *CRC Press, 2009, ch. 22, pp. 523–584.*

[8] B. Marchon and Y. Saito, "Lubricant Thermodiffusion in Heat Assisted Magnetic Recording," *IEEE Transactions on Magnetics, vol. 48, no. 11, pp. 4471–4474.* 2012.

[9] L. Wu, "Modelling and simulation of the lubricant depletion process induced by laser heating in heat-assisted magnetic recording system," *Nanotechnology, vol. 18, p. 215702.* 2007.

[10] H. Matsuoka, K. Oka, Y. Yamashita, F. Saeki, and S. Fukui, "Deformation characteristics of ultra-thin liquid film considering temperature and film thickness dependence of surface tension," *Microsystem Technologies, vol. 17, no. 5-7, pp. 983–990,* 2011.

[11] X.-C. Guo, B Knigge, B. Marchon, R. J. Waltman, M Carter, and J Burns, "Multidentate functionalized lubricant for ultralow head-disk spacing in a disk drive," *Journal of Applied Physics, vol. 100, p. 044 306.* 2006.

[12] J. B. Dahl and D. B. Bogy, "Lubricant Flow and Evaporation Model for Heat Assisted Magnetic Recording Including Functional End-Group Effects and Thin Film Viscosity," *Tribology Letters, vol. 52, no. 1, pp. 27–45.* 2013.

[13] C. M. Mate, "Spreading Kinetics of Lubricant Droplets on Magnetic Recording Disks," *Tribology Letters, vol. 51, no. 3, pp. 385–395.* 2013.

[14] R. J. Waltman, H. Deng, "Low Molecular Weight Z-Tetraol Boundary Lubricant Films in Hard Disk Drives," *Advances in Tribology Volume 2012, Article ID 964089*, 2012.

[15] "Fomblin Z Derivatives Product Data Sheet", Solvay Solexis, 2002